J Solid State Electrochem (2006) 10: 91–95
DOI 10.1007/s10008-005-0666-6

ORIGINAL PAPER

Gennady I. Ostapenko

Investigation of electrochemical reactions on copper electrode in $Cu_4RbCl_3I_2$ solid electrolyte

Received: 28 September 2004 / Revised: 13 January 2005 / Accepted: 10 March 2005 / Published online: 20 May 2005
© Springer-Verlag 2005

Abstract Investigations are carried out by potentiostatic method. It is found that at potentials φ less than 100 mV, a reaction rate of copper deposition is limited by the formation and the three-dimensional growth of copper nuclei and the rate of copper dissolution is limited by a two-dimensional growth of holes in the metal. The rate of nucleus growth was evaluated at 10^{-9}...10^{-6} μm s^{-1} depending on the potential. At $\varphi > 120$ mV, the reaction rate is limited by charge transport at the exchange current density of 2.7 mA cm^{-2} and the anodic transfer coefficient $\alpha_a \approx 0.45$. The accumulation of a divalent copper phase on $Cu/Cu_4RbCl_3I_2$ interface at anodic polarization is explained by a parallel course of $Cu^+ - e \rightarrow Cu^{2+}$ reaction.

Keywords Solid electrolyte · Rubidium tetracopper trichloride diiodide · Copper electrode · Electrode kinetics · Slow electrocrystallization

Introduction

Extensive experimental data on the kinetics of electrochemical processes on a copper electrode in Cu^+-conducting solid electrolytes have been accumulated. As shown in work [1], a layer of cuprous oxide, Cu_2O, occurs on the interface of the copper electrode with $Cu_4RbCl_3I_2$. At $\varphi < 8$–10 mV, this layer blocks the course of the electrochemical reaction:

$$Cu^0 - e \leftrightarrow Cu^+ \quad (1)$$

with participation of metal copper, and the copper electrode behaves as inert. At the same time it is known, that Cu^+-conducting solid electrolytes always contain Cu^{2+}-impurity [2, 3]. Therefore under these conditions, on the copper electrode the following electrochemical reaction with Cu^{2+} participation takes place:

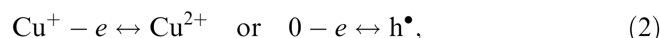

$$Cu^+ - e \leftrightarrow Cu^{2+} \quad \text{or} \quad 0 - e \leftrightarrow h^\bullet, \quad (2)$$

where $h^\bullet$ is an electronic hole. The rate of this reaction is limited by slow diffusion Cu^{2+} or electronic holes in $Cu_4RbCl_3I_2$ [1].

An electrical breakdown of oxide layer at potentials $\varphi > 8$–10 mV takes place and the reaction (1) with participation of metal copper is deblocked [1]. However, a clear interpretation of this reaction kinetics does not exist. For example, in works [4, 5] it is affirmed that crystallization effects are the limiting stage of electrode reaction at potentials higher than 30 mV. However, in work [6] it is affirmed, that the electrocrystallization cannot be the limiting stage. In work [7] it is shown, that a divalent copper phase is accumulated on the copper electrode surface at considerably high anodic polarization, however, interpretation of this phenomenon does not exist.

The present work investigates in detail the copper dissolution—deposition kinetics on the $Cu/Cu_4RbCl_3I_2$ interface by a potentiostatic method.

Experiment

The $Cu_4RbCl_3I_2$ solid electrolyte was prepared by the method given in work [1]. The surface of a flat copper electrode was hand-ground by corundum powders of various dispersions, polished by diamond paste to a smooth surface, cleaned by ethanol and CaO + MgO aqueous paste and washed with water. The electrodes were annealed at 500 °C under a pressure 10^{-2} Pa for 6 h and slowly cooled to room temperature.

Cells of the type $Cu/Cu_4RbCl_3I_2/Pt$ were prepared in dry air (utilizing P_2O_5 as dehydrator) by subjecting the

Presented at the conference Solid State Chemistry 2004, September 13-17, Prague, Czech Republic

G. I. Ostapenko
Togliatti State University,
Belorusskaya St., 14, Togliatti,
445667, Russia
E-mail: gostap@tltsu.ru

electrolyte powder to a pressure of 2.2×10^{8} Pa. The thickness of the electrolyte layer was about 1 mm. The copper wire reference electrode of 0.2 mm diameter was positioned in the middle of the electrolyte. Working copper and platinum counter electrodes were placed on the electrolyte layer surfaces. The cells were compressed in a special equipment under a load of about 3×10^{6} Pa, annealed at 160 °C for 3 h and cooled slowly to room temperature.

All electrochemical measurements were carried out at 25 °C using P-5848 potentiostat (Russia), as described elsewhere [8]. The low currents were measured using a sensitive TR-1452 current-voltage follower (Hungary).

Results and discussion

Applicability of equations for classical electrochemical kinetics to solid-state systems is discussed [9, 10]. It is shown [11] that the slow diffusion of conducting ions has no place in unipolar solid electrolytes. R.D. Armstrong [12] shows that slow crystallization and charge transport across electrode–electrolyte interface take place in such conditions. These processes are also described by classical equations which are applied to liquid electrochemical systems. Therefore, in the present work these equations are used.

Electronic conduction takes place in the investigated $Cu_4RbCl_3I_2$ solid electrolyte (1.2×10^{-7} Sm cm^{-1} [1]). However, the value of electrolyte electronic conductivity between working and reference electrodes (≈10^{-6} Sm) is much less than the general conductivity of the cell (≈10^{-3} Sm, for example from Fig. 1). The influence of electronic conduction on the measurement results can therefore be neglected.

A potential drop in electrolyte between working and reference electrodes does not exceed one percent from overvoltage which feeds these electrodes. Therefore distortions of overvoltage can be neglected in these conditions.

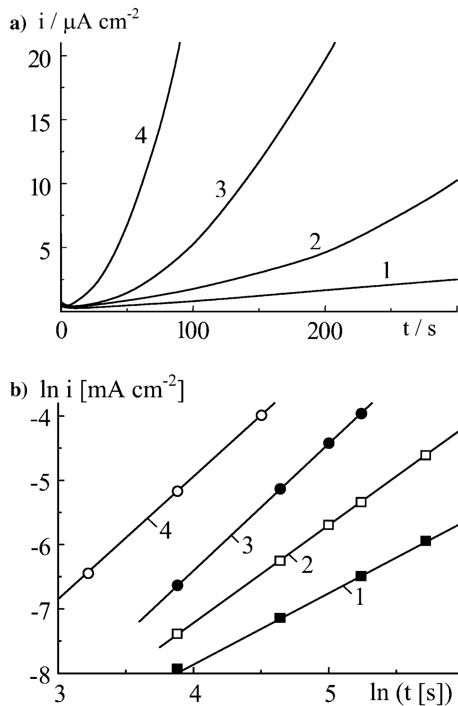

Fig. 1 Potentiostatic transients for copper anodic dissolution at low potentials, (mV) *1*: 15; *2*: 18; *3*: 20; *4*: 22

Anodic dissolution of copper

In Fig. 1a potentiostatic transients for copper anodic dissolution at low potentials are shown. These transients are typical for the formation and growth of holes on the metal surface. The initial sites of such transients are described by $I\infty t^n$ dependence, where n determines the law of formation and growth of holes [13]. The n value can be estimated from line slopes in Fig. 1b. As is seen in Fig. 2, n increases approximately from 1 to 2 with increasing potential. Two-dimensional growth of holes takes place mainly at anodic dissolution [14]. Hence, at rather low potentials and short times, the current varies according to the law [13]:

$$I = \pi q N_0 V_1^2 t,$$

where q is the dissolving layer charge, N_0 is the quantity of the instantaneously formed holes and V_1 is the advance rate of the dissolution front along the electrode surface. Apparently, at higher potentials, along with instantaneously formed holes, new holes with rate A are formed. Consequently, the law of the current change with time tends to square-law [13]:

$$I = \pi q V_1^2 A t^2 \tag{3}$$

Figure 3a shows potentiostatic transients at medial potentials. On these transients, the current initial overshoot is caused, apparently, by double layer charging and relaxation of minority charge carriers. Here also we disregard it. It is seen that with the potential increase, the dependence of the current on time becomes less expressed, and at potentials higher than 120 mV, as evident from Fig. 3b, this dependence generally disappears (In Fig. 3b the declination front slope of transients is

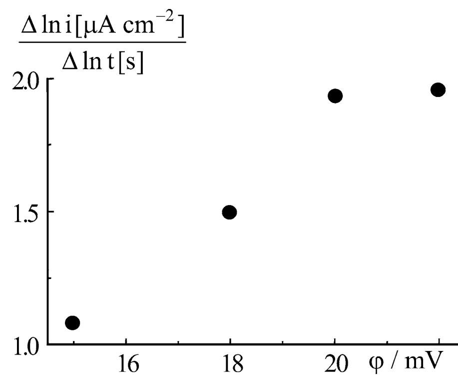

Fig. 2 $n = \Delta\ln\ I/\Delta\ln\ t$ slopes of lines from Fig. 1b

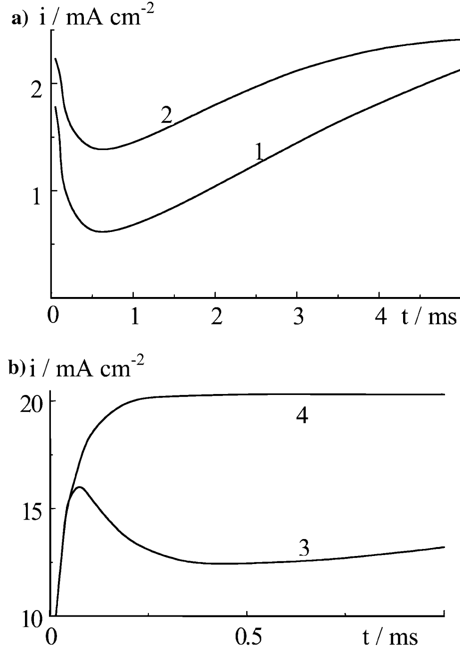

Fig. 3 Potentiostatic transients for copper anodic dissolution at medial (**a**) and high (**b**) potentials, (mV) *1*: 40; *2*: 50; *3*: 100; *4*: 120

caused by potentiostat speed). Hence, at potentials higher than 120 mV, the copper anodic dissolution is limited by slowed charge transfer. Accordingly, in Fig. 4 it is seen that anodic current-voltage characteristic (CVC) (this CVC is constructed according to "saddles" and established current values, for example from Fig. 3) at these potentials is described by the equation [14]:

$$\ln\frac{i}{1-\exp(e/kT)\eta}=\ln i_0\alpha\frac{e}{kT}\eta \tag{4}$$

with the exchange current density $I_0 = 2.7$ mA cm^{-2} and anodic transfer coefficient $\alpha_a \approx 0.45$.

Cathodic deposition of copper

In Fig. 5a potentiostatic transients for copper cathodic deposition are shown at low potentials and short times.

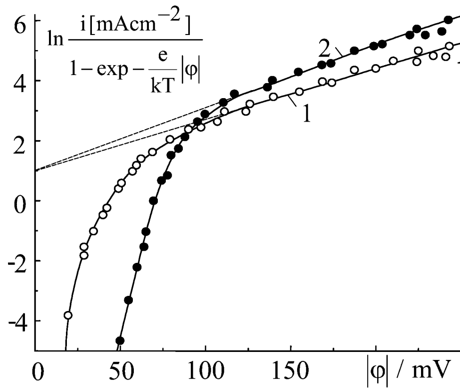

Fig. 4 Current-voltage characteristics of the copper electrode: *1* anodic, *2* cathodic

From these transients in logarithmic coordinates (Fig. 5b) it follows that the value of n, which determines the law of the current change with time, is 1.9 ± 0.1. Hence, the copper deposition can be determined by progressing formation and two-dimensional growth of nuclei according to Eq. 3 or instantaneous formation and three-dimensional growth of nuclei [13]:

$$I=\frac{e\rho}{m_0}V_1^2V_2\pi N_0t^2, \tag{5}$$

where V_2 is the growth rate of nuclei perpendicular of the electrode surface.

It is known that the reversible and inert electrodes in solid electrolytes behave identically as regards cathodic deposition [15]. Besides, the growth of needles and dendrites is observed at deposition [16, 17]. These facts suggest that copper is deposited on copper according to Eq. 5 with instantaneous formation and three-dimensional growth of nuclei, i.e. needles and dendrites.

In the formation and three-dimensional growth of nuclei and at time tending to zero [13]:

$$i_{t\to 0}=\frac{e\rho}{m_0}V_3, \tag{6}$$

where V_3 is the growth rate of thickness of the electrode starting sheet. For longer times [13]:

$$i_{t\to\infty}=\frac{e\rho}{m_0}V_2. \tag{7}$$

As seen in Fig. 5a, current $i_{t\,\to\,0} \approx 0$ at low potentials. Hence, the electrode thickness is not incremented, but the needles and dendrites grow intensively on its

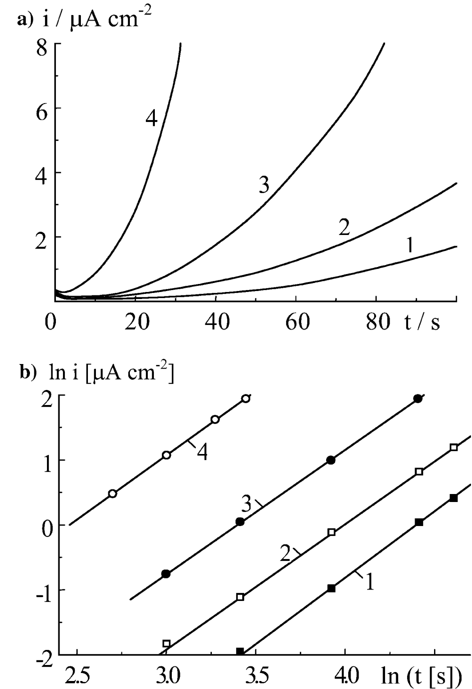

Fig. 5 Potentiostatic transients for copper cathodic deposition at low potentials, mV: *1* (−10); *2* (−11,5); *3* (−13); *4* (−14,5)

surface. This current flows and increases with increasing potential (Fig. 6). Figure 7 shows the dependence of V_2 and V_3 calculated according Eqs. 6 and 7 on the potential. According to this figure the growth rate of needles and dendrites greatly exceeds the growth rate of the deposit thickness at rather low potentials. The difference of rates is reduced with increasing potential; they are also compared at potentials higher than 80–100 mV. Hence, at these and higher potentials the needles and dendrites practically do not grow, and the thickness of the starting sheet is increased.

The quantity of nuclei increases with increasing potential [13]. At some value of the potential the quantity of nuclei cannot increase, since each atom on the electrode surface will be a nucleus. Therefore, dissolution and deposition of copper should be limited by slow charge transfer at the above indicated potentials. Actually, in Fig. 4 we see that the CVC of copper deposition at potentials higher than 120 mV is described by Eq. 4 at $i_0 = 2.7$ mA cm^{-2} and cathodic transfer coefficient $\alpha_c \approx 0.55$.

Cathodic and anodic CVCs significantly differ at potentials below 100 mV (Fig. 4), i.e. their considerable asymmetry is observed. It is caused, apparently, by various mechanisms of crystallization, since at anodic dissolution two-dimensional growth of holes takes place, and at cathodic deposition—mainly three-dimensional growth of needles and dendrites.

Apparently, the reaction (2) flows parallel with reaction (1) at high potentials. Therefore, under these conditions the electrode reaction (2) takes place for generating the electronic holes at anodic polarization. The electrolyte stoichiometry changes as a result into the near—electrodic zone:

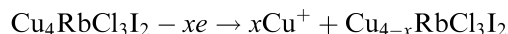

$$Cu_4RbCl_3I_2 - xe \rightarrow xCu^+ + Cu_{4-x}RbCl_3I_2$$

Nonstoichiometry increases with increasing potential and reaches electrolyte homogeneity limit at the electrolyte electrochemical decomposition potential of 0.58 V [18] and the divalent copper phase is deposited on the electrode.

It is necessary to notice that the cuprous oxide layer on the copper electrode surface influences electrode

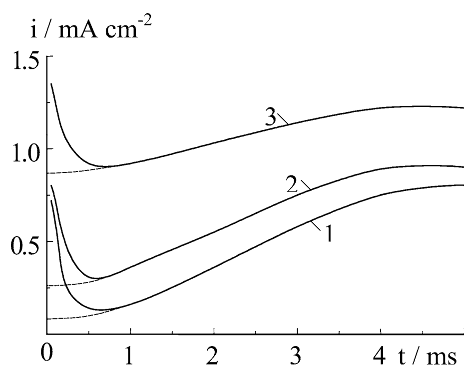

Fig. 6 Potentiostatic transients for copper cathodic deposition at medial potentials, mV: *1* (−60); *2* (−65); *3* (−70)

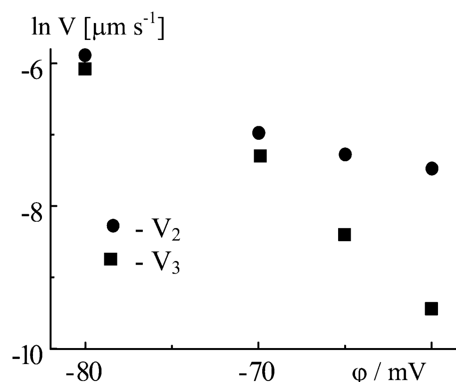

Fig. 7 Dependence of the growth rate of needles and dendrites (V_2) and growth rate of the starting sheet thickness (V_3) of copper on the potential

behaviour at potentials less than 10 mV. At higher potentials this layer is destroyed at electrical breakdown, and the CVCs practically coincide [6] irrespective of the presence or absence of the cuprous oxide layer.

Conclusions

The rate of copper deposition is limited by the formation and three-dimensional growth of copper nuclei and the rate of copper dissolution is limited by the growth of two-dimensional holes in the metal at potentials less than 100 mV. The rate of nucleus growth was evaluated at $10^{-9}...10^{-6}$ μm s^{-1} depending on potential.

At $|\varphi| > 120$ mV, the reaction rate is limited by charge transfer at $i_0 = 2.7$ mA cm^{-2} and anodic transfer coefficient of approximately 0.45.

The accumulation of the divalent copper phase on the copper electrode surface at anodic polarization is explained by a parallel course of $Cu^+ - e \rightarrow Cu^{2+}$ reaction.

References

1. Ostapenko GI, Cox A, Ostapenko LA (2002) J Solid State Electrochem 6:245
2. Nimon E, L'vov A, Senotov A, Demakhin A, Pridatko I (1984) Neorgan Mater USSR 20:670
3. Ostapenko GI (1999) Ionics 5:316
4. Armstrong RD, Dickinson T, Taylor K (1974) J Electroanal Chem 57:157
5. Kukoz FI, Kolomoets AM, Kuz'min VP (1980) Elektrokhimiya 16:1861
6. Vershinin NN, Malov Yu I, Ukshe EA (1982) Elektrokhimiya 18:255
7. Yushina LD, Kochergina LV, Gromov OG (1986) Elektrokhimiya 22:1223
8. Kolomoets AM, Ostapenko GI (1980) Elektrokhimiya 16:379
9. Itskovich EM, Kornyshev AA, Vorotyntsev MA (1977) Phys Stat Solidi (a) 39:229
10. Kornyshev AA, Vorotyntsev MA (1981) Electrochim Acta 26:33
11. MacDonald JR (1975) J Appl Phys 44:3455
12. Armstrong RD, Dickinson T, Willis PM (1975) J Electroanal Chem 59:281

13. Harrison JA, Thirsk H (1971) In: Bard AJ (ed) Electroanal Chem, vol 5. Decker, New York, p 67
14. Vetter KJ (1961) Elektrochemische Kinetik. Springer, Berlin Goettingen Heidelberg New York
15. Scrosati B (1985) In: Solid state batteries. Proceedings of the NATO Advanced Study Institute, Alcabideche, 2–14 September 1984, Dordrecht e.a., p 109
16. Schemilt JM, Steele BCH, Weston JE (1981) Solid State Ionics 2:1
17. Warner TE, Edwards PP, Timms WC (1992) J Solid State Chem 98:415
18. Ostapenko GI (2001) J Solid State Electrochem 5:393